

FINAL MISSION AND NAVIGATION DESIGN FOR THE 2016 MARS INSIGHT MISSION

Fernando Abilleira^{*}, Allen Halsell[†], Ken Fujii[‡], Eric Gustafson[§], Clifford Helfrich^{}, Eunice Lau^{††}, Julim Lee^{‡‡}, Neil Mottinger^{§§}, Jill Seubert^{***}, Evgeniy Sklyanskiy^{†††}, Mark Wallace^{‡‡‡}, Jessica Williams^{§§§}**

NASA's Interior Exploration using Seismic Investigations, Geodesy, and Heat Transport (InSight) mission was scheduled to launch the next lander to Mars in March 2016 arriving to the Red Planet in the fall. Derived from the Phoenix mission which successfully landed on Mars in May 2008, the InSight Entry, Descent, and Landing system will place a lander in the Elysium Planitia region. This paper specifies the mission and navigation requirements set by the Project and how the final mission and navigation design satisfies those requirements. Background information affecting navigation including spacecraft modeling and the physical environment which influences the spacecraft motion are included. (Note from the author: The InSight launch in 2016 was suspended due to critical issues with the Seismic Experiment for Interior Structure (SEIS) instrument that could not be fixed prior to the planned launch period. This paper represents the state of the design for the 2016 mission. No attempt has been made to reflect the latest developments).

INTRODUCTION

The Interior Exploration using Seismic Investigations, Geodesy, and Heat Transport (InSight) Mission has the primary objective of placing a science lander on the surface of Mars followed by the deployment of two science instruments onto the Martian surface to investigate the fundamental processes of terrestrial planet formation and evolution. By performing the first comprehensive surface-based geophysical investigation of Mars, InSight will provide key information on the composition and structure of an Earth-like planet that has gone through most of the evolutionary stages of the Earth up to, but not including, plate tectonics.

The primary systems for the InSight project are the Flight System, the Mission System, the launch vehicle, and the ground stations of the Deep Space Network (DSN), the European Space Agency (ESA), and the Japanese Space Agency (JAXA). The Phoenix-heritage flight system consists of the cruise stage, the entry system, and the lander. The entry system consists of the backshell, parachute, and heat shield. The

^{*} InSight Mission Design & Navigation Manager, Fernando.Abilleira@jpl.nasa.gov

[†] InSight Navigation Team Chief, Charles.A.Halsell@jpl.nasa.gov

[‡] InSight Mission Engineer, Kenneth.K.Fujii@jpl.nasa.gov

[§] InSight Orbit Determination Lead, Eric.D.Gustafson@jpl.nasa.gov

^{**} InSight Maneuver Analyst, Clifford.E.Helfrich@jpl.nasa.gov

^{††} InSight Orbit Determination Analyst, Eunice.L.Lau@jpl.nasa.gov

^{‡‡} InSight Orbit Determination Analyst, Julim.Lee@jpl.nasa.gov

^{§§} InSight Orbit Determination Analyst, Neil.Mottinger@jpl.nasa.gov

^{***} InSight Orbit Determination Analyst, Jill.Tombasco@jpl.nasa.gov

^{†††} InSight Entry, Descent, and Landing Trajectory Analyst, Evgeniy.Sklyanskiy@jpl.nasa.gov

^{‡‡‡} InSight Trajectory Lead, Mark.S.Wallace@jpl.nasa.gov

^{§§§} InSight Maneuver Analyst, Jessica.Williams@jpl.nasa.gov

Jet Propulsion Laboratory, California Institute of Technology, 4800 Oak Grove Drive, Pasadena, CA 91109.

InSight mission will deliver the InSight lander to the surface of Mars in the 2016 Earth-Mars opportunity. The InSight spacecraft will be launched in March 2016 from Vandenberg Air Force Base (VAFB) in California on a United Launch Alliance (ULA) Atlas V 401 and will arrive at Mars in September 2016.¹

MISSION

Launch

InSight will be launched onto a ballistic, Type 1 trajectory using an Atlas V 401 launch vehicle (LV) from Space Launch Complex 3E (SLC-3E) at Vandenberg Air Force Base (VAFB) in California. The 27-day launch period extends from March 4 through March 30, 2016. The launch flight azimuth is maintained constant at 191 deg across the launch period. The Centaur first burn, which is the longer of the two Centaur upper stage firings, will inject the vehicle onto a ~185 km circular park orbit inclined at 109°. After coasting for 60 to 67 min, the Centaur/spacecraft stack will reach the proper position for the second Centaur burn to inject the spacecraft onto the desired departure trajectory. The launch window on any given day during the launch period has a duration of up to 120 min, depending on launch vehicle performance and the required injection energy. The launch vehicle injection targets are specified as twice the hyperbolic injection energy per unit mass (C3), declination of the launch asymptote (DLA), and right ascension of the launch asymptote (RLA) at the Targeting Interface Point (TIP), defined as Main Engine Cutoff #2 (MECO2) plus 10 min. The injected spacecraft mass is 700.5 kg. Propellant Margin (PM) defined as the additional burnable propellant beyond the Flight Performance Reserve (FPR), and Launch Vehicle Contingency (LVC), is used to create daily launch windows. In addition to the InSight spacecraft, two secondary payloads known as Mars Cubesat One (MarCO) are being considered to be launched with InSight. The MarCO spacecraft would provide a real time telemetry link between the InSight spacecraft and Earth during InSight's Entry, Descent and Landing (EDL) phase at Mars.

Interplanetary Cruise

During the 6.5-month interplanetary flight of the spacecraft, up to six planned trajectory correction maneuvers (TCMs) will be employed to remove the planetary protection-required aimpoint bias, correct any launch vehicle injection errors, and deliver InSight to its intended entry interface point (EIP). A plot of the heliocentric trajectory for the open of the launch period is shown in Figure 1. Also during the Cruise phase, telecom, attitude control, navigation, and lander capabilities to be used during the Entry, Descent, and Landing (EDL) and surface phases will be checked out. The science payload will have a checkout opportunity during the Early Cruise sub-phase. The spacecraft will require pointing updates to maintain antenna pointing near Earth and the solar panels pointing toward the Sun as their relative positions change during

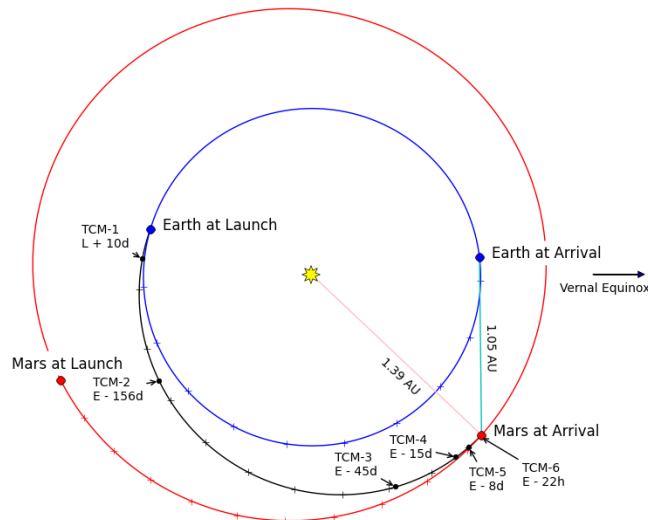


Figure 1. Interplanetary Trajectory for launch on 03/04/2016

flight. The Approach sub-phase includes the acquisition and processing of navigation data needed to support the development of the final four trajectory correction maneuvers (TCM-3 through TCM-6), the spacecraft activities leading up to separation of the entry vehicle from the cruise stage, and the final turn to the entry attitude. The last four TCMs are used to perform final adjustments to the incoming trajectory at Mars to ensure that the desired entry conditions are achieved. All other spacecraft activities, particularly those

that could influence the spacecraft’s trajectory (e.g., a spacecraft attitude turn), are minimized. During the Approach sub-phase, the amount of requested DSN tracking is substantially increased to allow more accurate trajectory solutions to be determined in the final weeks before arrival at Mars. In addition to increased Doppler and ranging data, additional Delta Differential One-way Ranging (Δ DOR) measurements are also taken during this period to ensure an accurate delivery at Mars.

Several days prior to entry, the EDL sequence is loaded on-board the spacecraft and begins executing. This sets a clock running which will bring about the sequence of activities that enable the EDL phase. A final TCM opportunity, along with a contingency TCM during the last 24 hours, may be used to make final corrections to target the Mars atmospheric Entry Interface Point (EIP). Approximately seven minutes before encountering the Martian atmosphere, the Cruise stage is jettisoned from the entry vehicle, and communication via Ultra-High Frequency (UHF) to Earth and to the Mars Reconnaissance Orbiter (MRO) commences. The TCM profile is shown in Table 1.

Event	Location (Days)	Objectives
TCM-1	L + 10	Removes launch vehicle targeting bias and injection errors, potentially targets to Entry Interface Point (EIP) defined for specific launch date. TCM-1 includes a deterministic component required to remove the launch vehicle aimpoint bias.
TCM-2	E - 156	Statistical maneuver to correct for orbit determination errors and TCM-1 execution errors; targets to EIP for specific launch date (accounting for predicted Thruster Calibration).
Thruster Calibration	E - 127	Thruster Calibration induces a small velocity change which is accounted for in TCM-1 and TCM-2 design.
TCM-3	E - 45	Statistical maneuver to correct for orbit determination errors, TCM-2 execution errors and variations due to the Thruster Calibration; targets to EIP for specific launch date.
TCM-4	E - 15	Statistical maneuver to correct for orbit determination errors and TCM-3 execution errors; targets to EIP for specific launch date.
TCM-5	E - 8	Statistical maneuver to correct for orbit determination errors and TCM-4 execution errors; targets to EIP for specific launch date.
TCM-5X	E - 5	Contingency maneuver. Same objectives as TCM-5. Performed only if TCM-5 is not executed nominally.
TCM-6	E - 22	Statistical maneuver to correct for orbit determination errors and TCM-5/5x execution errors; targets to EIP for specific launch date.
TCM-6X	E - 8	Contingency maneuver. Final opportunity for entry targeting maneuver. Performed only if TCM-6 does not take place (TCM-6X designed with TCM-6).
TCM-6XM	E - 8	Contingency maneuver. Final opportunity for entry targeting maneuver. Will be selected from menu of validated maneuvers to maximize the probability of successful landing.

Table 1. TCM Profile

Entry, Descent, and Landing (EDL)

The entry vehicle then begins its turn to entry attitude six and one-half minutes before entering into the Martian atmosphere. This atmospheric Entry Interface Point is defined to occur at a radius of 3,522.2 km from the center of Mars and represents the point at which atmospheric effects are first expected to be sensed by the spacecraft. Following this direct entry into the Martian atmosphere, the entry vehicle rapidly decelerates due to drag from its hypersonic entry velocities to supersonic parachute deployment velocities as it passes through the increasingly dense atmosphere. The onboard flight software parameters are optimized in order to guarantee that in the presence of EDL error sources, the chute deployment occurs within the established Mach/dynamic pressure limits driven by a maximum parachute opening load of 15,000 lbf. The heatshield is jettisoned after the parachute has opened, followed later by the power up of the landing radar and the deployment of the lander legs. The radar will be used during the terminal descent phase to

provide input to the descent engines that are then fired to further slow the spacecraft down and land gently on the Martian surface.

Cruise phase navigation and maneuver design will target the E09 ellipse located in the Elysium Planitia region (areocentric latitude = 4.460 deg, East longitude = 135.970 deg).² Note that all trajectories target the E09 reference site on launch day 1 at the launch window open as illustrated in Figure 2. This Figure also shows the landing ellipse azimuth variation across the launch period. The final site has been subjected to extensive reconnaissance by MRO instruments over the years leading to launch.

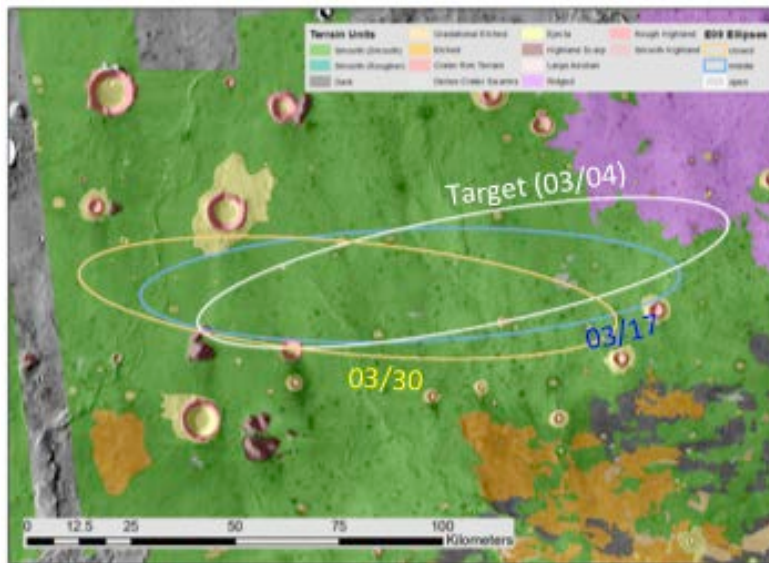


Figure 2. Landing Ellipse Variation across Launch Period

Surface

Once safely on the surface of Mars, the lander is configured for Surface operations. The solar arrays are deployed. Science and engineering data acquired during EDL and during the first hour on the surface will be transmitted to Earth via the lander-to-orbiter UHF-relay link to assess the state of the lander and to ensure that it has achieved a power/thermal safe state. The Instrument Deployment sub-phase commences once it has been determined that the solar arrays are deployed and the lander is in a safe and communicative state. For the first several sols on the surface, the lander and its surrounding environment, including the workspace, are characterized, the payload elements are checked out, the initial weekly Rotation and Interior Structure Experiment (RISE) measurements are acquired, and the critical data collected on Sol 0 – the landing sol – continue to be relayed back to Earth. After the Science team has selected suitable deployment sites within the workspace, the Instrument Deployment Arm places the Seismic Experiment for Interior Structure (SEIS) and Heat Flow and Physical Properties Package (HP3) instruments on the Martian surface. Then, with both instruments in their final positions on the surface of Mars, and with SEIS collecting its science data, the HP3 mole is released. Once the flight team has confirmed that the HP3 mole has been released, the Penetration sub-phase begins. During this phase, the mole is allowed to penetrate the Martian regolith until it reaches its final depth over the course of about 30 sols. SEIS and HP3 acquire Science data throughout this phase, and RISE measurements continue to be acquired.

The Science Monitoring sub-phase starts at the conclusion of the Penetration sub-phase. SEIS, HP3, and RISE continue to collect science data throughout this phase. Science monitoring continues for one Mars year plus 40 sols after landing, with the possibility of extended surface operations continuing for as long as there is adequate power and funding.

SPACECRAFT

The InSight flight system design is based heavily on the Lockheed Martin-built Phoenix flight system that successfully landed on the surface of Mars in May of 2008. The InSight spacecraft is highly centralized and designed around a core lander that controls all functions throughout all mission phases. Three secondary flight elements (the cruise stage, heatshield, and backshell) provide the additional functions needed for Cruise and EDL. Figure 3 shows an expanded view of the InSight flight system. The mass allo-

cation for the entire flight system, including propellant, is 700.5 kg. The InSight lander contains all of the avionics, power electronics, and propulsion system. Most of the Guidance and Navigation Control hardware is located in the lander, augmented during cruise by redundant star trackers and sun sensors mounted on the cruise stage.

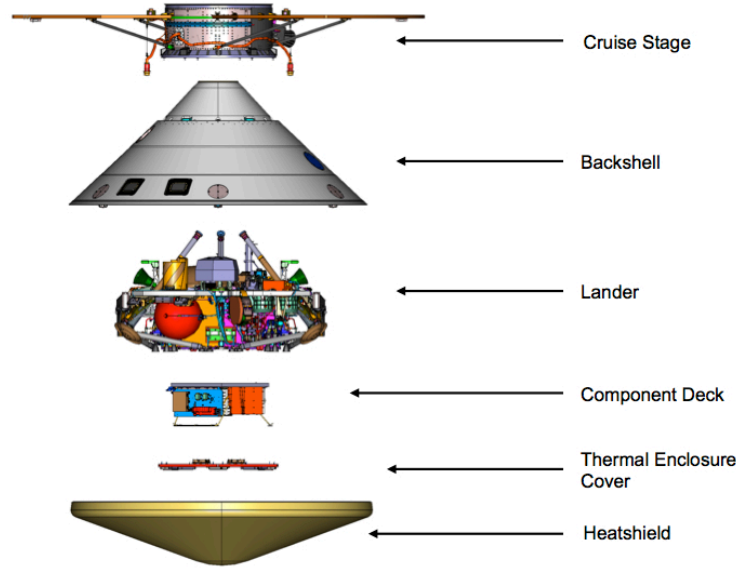


Figure 3. InSight Flight System – Expanded View

The majority of the telecommunications hardware is located on the lander, but during cruise an additional X-band transponder and dual amplifiers located on the cruise stage provide redundant X-band communications. The Cruise stage also provides power during cruise via two fixed wing arrays. The backshell and heatshield provide protection for the lander during entry, and the backshell houses the parachute that will slow the entry system prior to terminal descent. Figure 4 shows the flight system in cruise configuration.

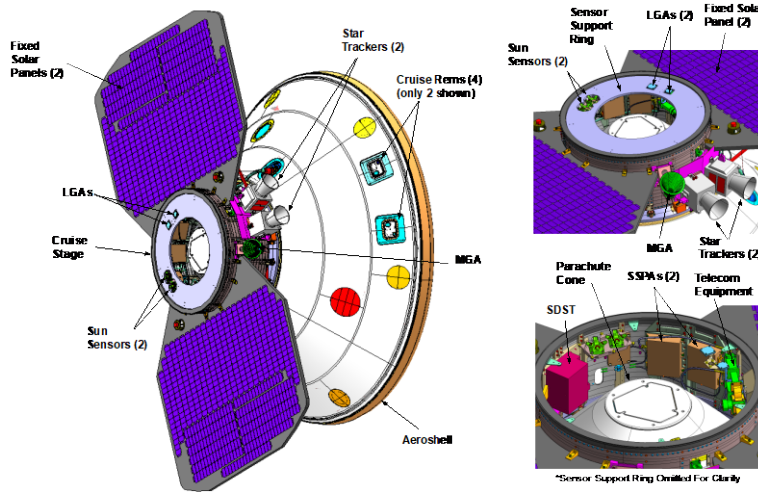


Figure 4. InSight Flight System – Cruise Configuration

Propulsion System

The lander propulsion system performs all cruise and EDL propulsion functions. Rocket Engine Modules (REMs) are scarfed through the aeroshell to allow Reaction Control System (RCS) and cruise TCM functions. Specifically, the system consists of four 1-lbf (4.4-N) RCS thrusters to provide attitude control, four 5-lbf (22-N) TCM thrusters to provide ΔV maneuvers during cruise, and twelve 68-lbf (302-N) descent engines to allow for EDL deceleration and attitude control. This configuration, including scarf and REM seal designs, was proven through extensive testing and the Phoenix flight.

Telecom System

The cruise telecommunications subsystem comprises fully redundant X-band Small Deep-Space Transponders (SDSTs) and Solid-State Power Amplifiers (SSPAs). It provides redundant transmit and receive capability through a fixed, dual-frequency, medium-gain horn and two low-gain patch antennas (one transmit, one receive). To accommodate the radio science experiment, one of the SDSTs was moved from the Cruise Stage to the Lander and an SSPA was added, both inside the thermal enclosure. Two fixed Medium Gain Antennas (MGAs) provide redundancy during landed operations.

During EDL, a UHF transceiver relays critical-event data to MRO and back to Earth. Prior to backshell separation, a wrap-around antenna on the backshell provides coverage, this is followed by the use of a helix antenna during terminal descent. During landed operations, the UHF transceiver performs relay operations to Mars orbiting assets from the lander twice per day on average. During EDL, two MarCO spacecraft (if launched as a secondary) would provide 8 kbps near real-time bent-pipe communications.

Attitude Control System

The spacecraft Attitude Control System (ACS) consists of two star trackers, two Miniature Inertial Measurement Units (MIMU), and Sun sensors. The primary attitude determination is done via the star trackers and the MIMU system. The analog Sun sensors serve as a backup system. Unlike the MSL (Mars Science Laboratory) spinning-stabilized attitude control strategy, the InSight spacecraft is three-axis stabilized via an unbalanced thruster control system. The RCS thrusters are fired intermittently to maintain a pre-determined deadband attitude profile. Additionally, the RCS thrusters are used to maintain attitude during TCMs (roll only) and safe-mode (3-axis control). The TCM ΔV and pitch/yaw control are performed by the TCM thrusters.

Attitude Deadbanding

Since the InSight spacecraft is three-axis stabilized, its attitude is not fixed. The attitude will vary within a set of deadbanding constraints defined by spacecraft telecom, power and thermal subsystems. ACS will command the thrusters to fire each time the attitude reaches one side of the deadband. The deadbands per axis [x, y, z] are [10, 10, 7.5] deg before 05/12/16, and are reduced to [4, 4, 4] deg from 05/12/16 to the slew to Entry.

Cruise Attitude

The cruise attitude strategy is to maintain the -X-axis pointed between the direction to the Earth and direction to the Sun. This strategy allows a telecom link to Earth using the Low Gain Antenna (LGA) or MGA antenna while providing sufficient power for spacecraft operations. The Cruise phase for InSight is divided into early Cruise and late Cruise. The transition from early to late Cruise will take place on 05/12/16. This transition date is fixed for all launch opportunities. In early Cruise, the LGA is used and the spacecraft attitude is such that the -X-axis face (solar array normal) of the solar arrays is offset 50 degrees from the Sun. This is driven by spacecraft thermal constraints. This configuration puts the MGA in the Sun/Earth plane. During this period, the LGA will be used for communications. For late Cruise, communications are switched to the MGA and the spacecraft -X-axis is pointed in the direction of the Sun.

REQUIREMENTS

The key and driving requirements for mission and navigation design are listed below:

The launch/arrival strategy shall...

Launch/Arrival Strategy and EDL Coverage

- ... launch between the dates of March 4 and March 30, 2016 both inclusive.
- ... support a Mars arrival of September 28, 2016.
- ... approach EDL with a V-infinity upper limit of 3.941 km/s.
- ... land in a region bounded by 5°N to 3°N.

EDL Coverage

- Mission Design and Navigation (MDNAV) shall design a spacecraft trajectory that provides line of sight to the Earth from cruise stage separation to touchdown plus 60 s.
- MDNAV shall design a spacecraft trajectory that has the capability to support UHF-band telecommunications with the Mars Reconnaissance Orbiter from Entry through touchdown plus 60 s.

TCM ΔV

- MDNAV shall assume that the cumulative ΔV_{99} for all Trajectory Correction Maneuvers (TCMs) targeted to the nominal landing site shall not exceed 30 m/s.

Atmospheric Entry Delivery/Knowledge Accuracies

- The entry vehicle shall approach EDL with an Entry Flight Path Angle (EFPA) of $-12.5 \text{ deg} \pm 0.21 \text{ deg}$, 3σ .
- MDNAV shall provide a final update to the entry state (known as the knowledge state) with a 3σ Entry Flight Path Angle uncertainty of $\pm 0.21 \text{ deg}$ and a 3σ entry time uncertainty of $\pm 0.15 \text{ s}$ not later than the last TCM plus 3 hours.
- MDNAV shall design a trajectory that has the capability to land the spacecraft within a 150 km by 35 km ellipse with a probability greater than or equal to 99%.

Planetary Protection

- The injection aimpoint for launch shall be biased away from Mars such that the probability of the launch vehicle upper stage impacting Mars is less than 1.0×10^{-4} for fifty years after launch.
- The probability of non-nominal impact of Mars due to failure during the cruise phase shall not exceed 1.0×10^{-2} .

MISSION DESIGN

Launch/Arrival Strategy

The InSight launch/arrival strategy was designed to provide critical EDL communications via direct-to-Earth and the Mars Reconnaissance Orbiter (MRO) using the UHF link for landing sites between 5°N and 3°N . This design assumes that MRO will achieve a Local Mean Solar Time (LMST) node of $\sim 2:30 \text{ PM}$ at the time of EDL. The primary constraint in the design was that the hyperbolic excess velocity at arrival (VHP) be less than 3.941 km/s. This maps directly into the entry velocity, which is a parameter of particular interest to the EDL team. In addition, the declination of the launch asymptote (DLA) was also originally constrained to be within $\pm 51 \text{ deg}$ to enable a launch out of Cape Canaveral Air Force Station (CCAFS) without requiring a waiver and in order to avoid further launch vehicle performance degradation. As launch is occurring out of Vandenberg Air Force Base (VAFB) in California, the March 4th launch period open is now constrained by schedule considerations. The launch/arrival strategy selected is illustrated in Figure 5.

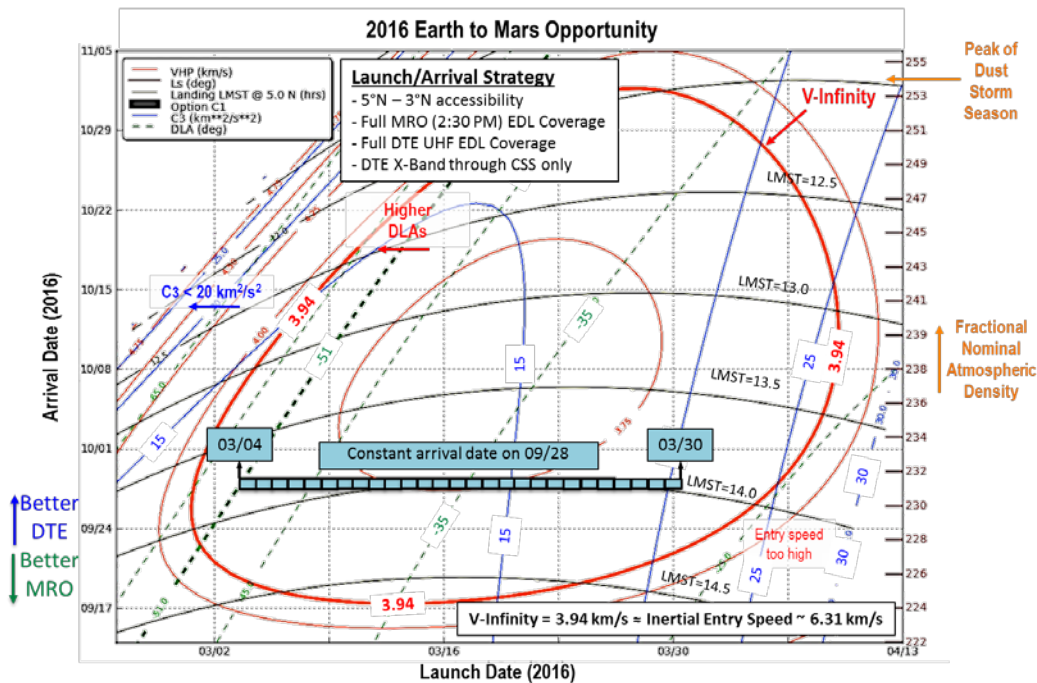


Figure 5. Launch/Arrival Strategy

Launch Period Characteristics

The launch vehicle targets represent the conditions of the osculating departure at the Targeting Interface Point (TIP) expressed in an Earth-center, inertial, Earth Mean Equator and Equinox of J2000 (EME2000) coordinate system. These Earth-relative target conditions are defined to occur 431 s after spacecraft separation from the upper stage of the launch vehicle and are shown in Table 2 along with the arrival V-infinity and arrival declination. The launch targets are held constant across the launch window for each day in the launch period and correspond to the optimal launch time for each launch day. The maximum C3 occurs at the close of the launch period, whereas the maximum DLA occurs at the open of the launch period. Assuming a spacecraft launch wet Maximum Possible Value (MPV) mass of 700.5 kg and based on the Atlas V 401 NASA Launch Services II contract data, the launch window duration is between 75 to 120 min.

Launch Day	Launch Date (2016, UTC)	Launch Window Duration (min)	Launch Opps	Earth Centered EME2000			IAU Mars Pole	
				C3 (km ² /s ²)	DLA (deg)	RLA (deg)	Arrival V-infinity (km/s)	Arrival Declination (deg)
1	03/04	120	25	11.980	-50.715	192.440	3.849	11.020
2	03/05	120	25	11.886	-49.280	193.120	3.828	10.222
3	03/06	120	25	11.841	-47.878	193.736	3.809	9.455
4	03/07	120	25	11.842	-46.512	194.301	3.793	8.717
5	03/08	120	25	11.887	-45.186	194.829	3.780	8.006
6	03/09	120	25	11.973	-43.903	195.330	3.768	7.320
7	03/10	115	24	12.098	-42.667	195.814	3.758	6.657
8	03/11	115	24	12.258	-41.482	196.284	3.750	6.015
9	03/12	110	23	12.452	-40.349	196.746	3.744	5.394
10	03/13	110	23	12.676	-39.271	197.199	3.739	4.792
11	03/14	105	22	12.927	-38.247	197.645	3.736	4.208
12	03/15	105	22	13.205	-37.275	198.082	3.734	3.640
13	03/16	105	22	13.508	-36.356	198.511	3.733	3.087
14	03/17	95	20	13.834	-35.487	198.931	3.733	2.549
15	03/18	95	20	14.184	-34.665	199.341	3.735	2.024
16	03/19	95	20	14.556	-33.891	199.744	3.737	1.513
17	03/20	90	19	14.950	-33.163	200.137	3.741	1.012
18	03/21	90	19	15.367	-32.482	200.522	3.745	0.523
19	03/22	90	19	15.806	-31.851	200.891	3.751	0.044
20	03/23	90	19	16.267	-31.273	201.228	3.758	-0.424
21	03/24	90	19	16.743	-30.714	201.492	3.765	-0.884
22	03/25	85	18	17.235	-30.087	201.734	3.773	-1.337
23	03/26	85	18	17.763	-29.463	202.071	3.783	-1.783
24	03/27	80	17	18.323	-28.905	202.442	3.793	-2.222
25	03/28	80	17	18.915	-28.405	202.821	3.804	-2.653
26	03/29	75	16	19.531	-27.933	203.178	3.816	-3.077
27	03/30	75	16	20.175	-27.489	203.528	3.829	-3.495

Table 2. Launch Targets and Arrival Characteristics

EDL Coverage

The selected launch period satisfies the requirement of maintaining full EDL communications from Entry to landing plus 1 min via both MRO and direct-to-Earth. It is assumed that EDL communications are available when the asset (MRO or Earth) has direct line of sight to InSight, i.e., InSight is not occulted by Mars as seen by the asset, and the antenna angle is within the antenna angle constraints. The antenna angle is defined as the angle between the atmosphere-relative anti-velocity vector and the line of sight to the asset. Even though, the resulting Parachute UHF (PUHF) antenna boresight actually points along the $-Z$ -axis, 6-DOF simulations indicate that the anti-velocity vector is a valid approximation to the modeling of the

-Z-axis direction during EDL. The antenna angle constraint is 135 deg. It is also required that the elevation angle from landing to landing plus 1 minute is at least 10 deg above the horizon line. Based on these constraints, a range of MRO mean anomalies at Entry Interface Point (EIP) has been identified. This range defines the orbital phasings from which MRO could provide EDL communication services. Given MRO's on-orbit phasing control of ± 30 s or ± 1.6 deg, only mean anomaly ranges of at least 5 deg are acceptable. This value includes margin to account for evaluation of EDL comm geometries using conic approximations.² In order to provide EDL communications coverage, on 07/29/15, MRO performed an inclination change maneuver to allow its ascending node to drift from 15:05 LMST through 14:30 LMST at the time of EDL. Upon reaching an ascending node of 14:27 LMST on 10/28/16 (Landing + 30 days), MRO will then perform another inclination maneuver to reverse its drift rate to return to a node of 15:00 LMST. On 04/06/17 (Landing + 190 days), a final inclination maneuver will be executed to halt this drift. ESA's Mars Express orbiter will also have visibility of the EDL event and will be recording the carrier signal. The Mars Odyssey and MAVEN orbiters have unfavorable geometry with respect to InSight and will not be able to provide EDL comm services. A technology demonstration known as Mars Cubesat One (MarCO) composed of two 14-kg 6U cubesats that would provide EDL comm support in near time is being considered. Figure 6 illustrates the arrival geometry.

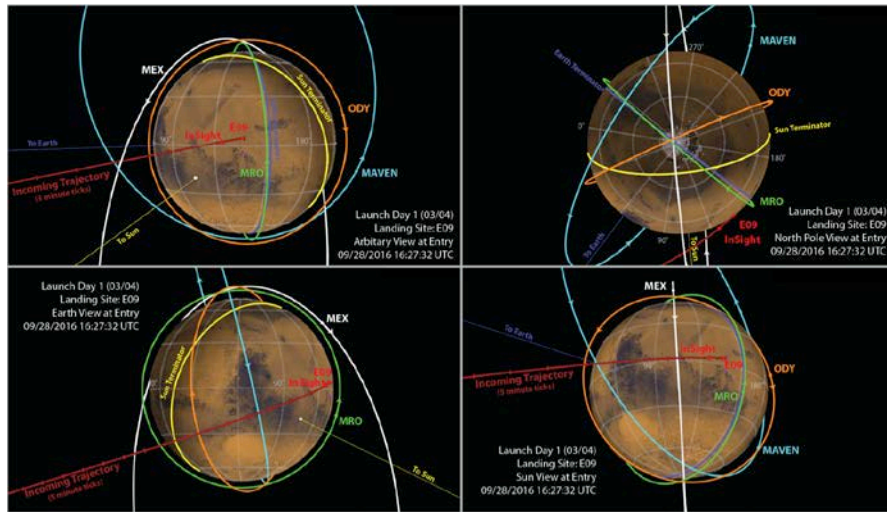


Figure 6. Arrival Geometry

NAVIGATION

Tracking Data

The baseline radiometric data types that will be used for InSight orbit determination are two-way coherent Doppler, two-way ranging, and Delta Very Long Baseline Interferometry (Δ VLBI) measurements generated by the DSN, ESA and JAXA for an X-band tracking system or a spacecraft to spacecraft UHF system. Doppler and ranging measurements are derived from a coherent radio link between the spacecraft and a receiver at a DSN ground station. Δ VLBI measurements will be acquired through DSN-DSN, DSN-ESA, ESA-ESA and DSN-JAXA baselines in the form of Delta Differential One-way Range (Δ DOR) measurements. The baseline Doppler, Range, and Δ DOR tracking scenarios are shown in Tables 3 and 4.

Phase	Relative Dates	Support
Cruise	Launch to L + 15 days	Continuous 34-m coverage
	L + 15 days to E - 60 days	Three 34-m 8-hour passes/week*
	L + 58 days to L + 74 days	One 34-m 8-hour pass/day**
	E - 64 days to E - 47 days	Two 34-m 8-hour pass/day
	E - 47 days to Entry	Continuous 34-m coverage
*Additional 4 days continuous coverage for TCMs + Thruster Calibration. **TCM-2 DCO		

Table 3. Baseline Doppler and Range Tracking Scenario

Spacecraft to spacecraft two-way coherent UHF Doppler will be generated by a link between the InSight spacecraft and a Mars orbiting spacecraft during the surface phase. For the navigation analysis reported in this document, the Δ DOR observable are assigned a metric data accuracy of 60 ps for DSN and JAXA and 120 ps for ESA ($1-\sigma$), and the quasar angular positions are assigned an uncertainty of 1 nrad ($1-\sigma$). Due to the transmission and processing time required for Δ DORs, InSight is using a 2-hour latency for DSN-DSN baselines and 24-hour for ESA-ESA, DSN-ESA and DSN-JAXA baselines.

Phase	Dates (UTC)	Stations	Number of Δ DOR	Duration (pre/post included)
Demonstration	23 June 2016 through 21 July 2016	NNO+CEB	3	2 hours
		GLD/CAN+MLG	3	
		CAN+USUDA	3	
Pre TCM-3	4 Aug 2016 through 8 Aug 2016	NNO+CEB	2	2 hours
		GLD/CAN+MLG	2	
		CAN+USUDA	2	
Pre TCM-4	17 Aug 2016 through 11 Sept 2016	NNO+CEB	6	2 hours
		GLD/CAN+MLG	6	
		CAN+USUDA	6	
Pre TCM-5	13 Sept 2016 through 18 Sept 2016	NNO+CEB	4	2 hours
		GLD/CAN+MLG	4	
		CAN+USUDA	4	
Approach	20 Sept 2016 through 27 Sept 2016	NNO+CEB	7	2 hours
		GLD/CAN+MLG	8	
		CAN+USUDA	7	
Total	45 ESA ΔDOR Passes (including demo passes): - Malargüe: 23 - Cebreros + New Norcia: 22 22 JAXA ΔDOR Passes (including demo passes) NNO = New Norcia, CEB = Cebreros, GLD = Goldstone, CAN = Canberra, MLG= Malargüe			

Table 4. Baseline Δ DOR Tracking Scenario

Attitude Maintenance Acceleration Uncertainty (Small Forces)

The small forces acceleration uncertainty is the acceleration equivalent of the uncertainty associated with the thrusting involved with attitude maintenance. Each time a thruster is fired to maintain the attitude inside predefined deadbands a small force or ΔV is imparted to the trajectory. It is important for the orbit determination (OD) process to model the error associated with these ΔV s. Because the spacecraft design is essentially a reflight of Phoenix, the covariance study has been using the in-flight data from Phoenix to calibrate the uncertainties associated with the small forces. The modeling of the deadbanding uncertainty is based on analysis of these data and is consistent with the following: (1) The bias in all directions is estimated and propagated as a prediction for future deadbanding, (2) the *a priori* uncertainty is set to $2.0e-11$ km/s², although it should be noted that the post-fit uncertainty in this term is greatly reduced with OD filtering and is not a significant source of error for prediction, and (3) the variations about the mean, as seen in the Phoenix data, are modeled with two different stochastic acceleration models.

- First, a white noise bias term is used to account for the short term pulse to pulse variations and the timing and number of actual thruster pulses in the future compared to the prediction. This term has been set to an a priori σ value of $2.25e-11$ km/s² for the spacecraft X-direction and $4.5e-12$ km/s² for spacecraft Y- and Z-directions.
- Long term effects observed in the data are modeled as a correlated noise process with a time constant of 14 days. The a priori uncertainty for those is $7.4e-12$ km/s² in the spacecraft X-direction and $1.5e-12$ km/s² in the spacecraft Y- and Z-directions.

Filter Configuration and Assumptions

The major error sources in orbit determination are TCM uncertainty and Δ DOR accuracy. The OD filter assumptions and error sources for the orbit determination results are shown in Table 5. In this table, “Est” indicates parameter estimation, “Stoch” indicates estimation with stochastics, and “Con” indicates consider covariance.

Error Source	Estimate	Uncertainties (1σ)			Comments
		Baseline	Degraded	No Margin	
2-way Doppler weight (mm/s)	-	0.1	0.2	0.05	
Range weight (m)	-	3	6	3	
DSN Δ DOR weight (ps)	-	60	120	60	
ESA Δ DOR weight (ps)	-	120	200	60	
JAXA Δ DOR weight (ps)	-	60	120	60	
DSN Δ DOR latency (hr)	-	2	17	2	Degraded value chosen to exclude last valid Δ DOR before TCM-6 DCO
ESA Δ DOR latency (hr)	-	24	48	12	Last valid MALA Δ DOR before TCM-6 DCO excluded in baseline & degraded
JAXA Δ DOR latency (hr)	-	24	48	12	
TCM and TCM Slews	Est	1.0 x Req.	1.2 x Req.	0.8 x Req.	Gates Model
Thruster Frame Y Direction (deg)	Est	3	Stoch = 3, Bias = 3	1	1 day update 0 correlation White Noise
Thruster Frame Z Direction (deg)	Est	3	Stoch = 3, Bias = 3	1	1 day update 0 correlation White Noise
Thruster Acceleration Magnitude Scale (%)	Stoch + Bias	Stoch = 5, Bias = 3	Stoch = 15, Bias = 3	Stoch = 5, Bias = 1	1 day update 0 correlation White Noise; Post-arc Stoch = 15%
Solar Pressure Scale Factor (%)	Stoch + Bias	Stoch = 3, Bias = 10	Stoch = 10, Bias = 10	Stoch = 3, Bias = 10	1 day update 7-day correlation ECRV (Exponentially Correlated Random Variable)
Range Bias (m)	Stoch	2	4	1	1 year update 0 correlation White Noise
Day Ionosphere (cm)	Con	55	75	27.5	No Margin MSL Performance
Night Ionosphere (cm)	Con	15	30	7.5	
Wet Troposphere (cm)	Con	1	2	0.25	
Dry Troposphere (cm)	Con	1	2	0.25	
X/Y Pole (cm)	Con	1	2	1	
UT1 (cm)	Con	2	4	2	
Station Locations	Con	2003 Cov	2003 Cov	2003 Cov	
Quasar Locations (nrad)	Con	1	2	0.5	
Mars GM (km^3/s^2)	Con	2.80E-04	2.80E-04	2.80E-04	
Earth-Mars Ephemeris scale	Con	1.0 x	2.0 x	0.5 x	
Earth GM (km^3/s^2)	Con	1.40E-03	1.40E-03	1.40E-03	
Moon GM (km^3/s^2)	Con	1.00E-04	1.00E-04	1.00E-04	
Deimos, Phobos Ephemeris	Con	1.0 x	1.0 x	1.0 x	

Table 5. Covariance Analysis Filter Assumptions

Cruise/Approach Navigation Accuracies

The orbit determination results presented in this section are based on the use of Doppler, range, and Δ DOR tracking data. They represent mappings of spacecraft state knowledge. The state uncertainty at the OD data cutoff (DCO) for each TCM design is mapped from the data cutoff time to the Mars-centered, Mars Mean Equator of Date B-plane at the time of Entry.

The OD data cutoffs for TCMs 1, 2, and 3 are 5 days before the respective maneuver. The OD data cutoffs for TCMs 4, 5 and 6 are 24 hours before the burns. The OD data arc used to compute the covariance for a given TCM design, depending on the circumstances, may or may not include the preceding TCM. The data arc for TCM-3 starts after TCM-2 and does not include TCMs 1 or 2. The data arcs for the approach TCMs 4, 5, and 6 start prior to TCM-3 (Entry-45 days) at 60 days before entry. TCM-6X would be attempted if, for whatever reason, TCM-6 could not be executed, and this maneuver was required to ensure that the atmospheric entry delivery accuracy requirements are met. Similarly, TCM-6XM would be executed if the additional tracking data following TCM-6/6X DCO indicated that the delivery accuracy requirements could not be met. Note that TCM-6X and TCM-6XM have the same execution time.

Figure 7 shows the associated mapping history of EFPA uncertainties with respect to DCOs for the DSN+ESA+JAXA Δ DOR case. As seen in this figure, the EFPA uncertainties meet the requirement about four days before the TCM-6 data cutoff. B-plane error ellipses resulting from the TCM-5 delivery, TCM-6 delivery and the corresponding knowledge statistics for the open, middle, and close of the launch period targeted to the E09 landing site for the baseline scenario are shown in Figures 8 through 10. The InSight B-plane delivery error ellipse is nearly circular due to the dominance of the TCM slew errors. A nearly circular B-plane error ellipse minimizes the B-plane angle's effect on the EFPA dispersion. As demonstrated in these figures, the EFPA uncertainties meet the requirement about four days before the TCM-6 data cutoff.

The EFPA delivery accuracy results from TCM-6 are given in Table 6. The table shows the variation in EFPA uncertainty for open, middle and close of the launch period and throughout the launch window for various Δ DOR combinations. In each case the use of non-DSN Δ DOR is clearly necessary to meet the EFPA requirement, and there is a small trend of increasing EFPA uncertainty for later launch dates.

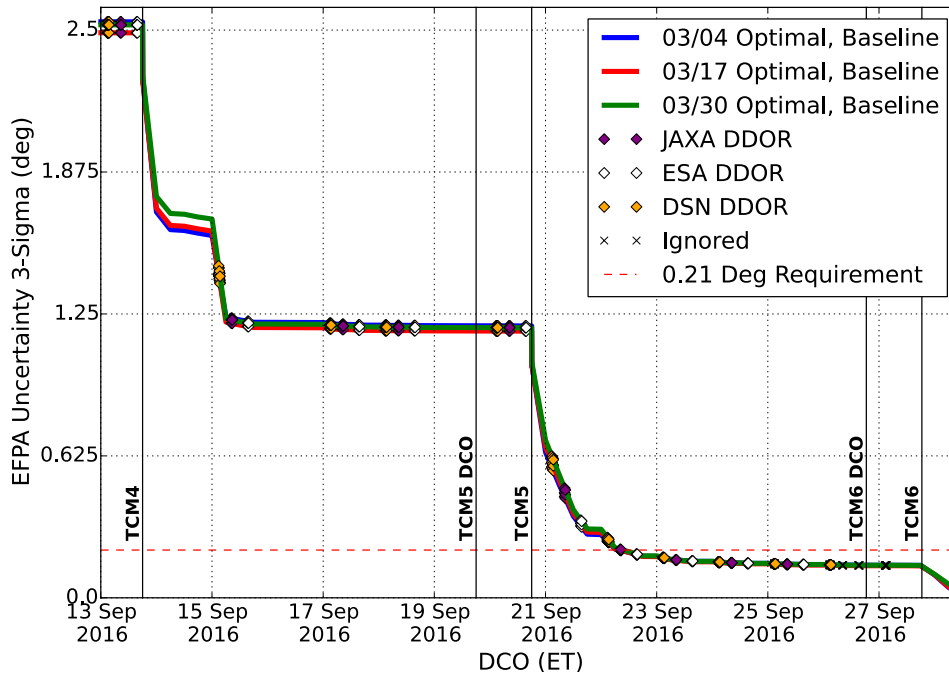


Figure 7. Evolution of EFPA Uncertainty with respect to DCO (Baseline)

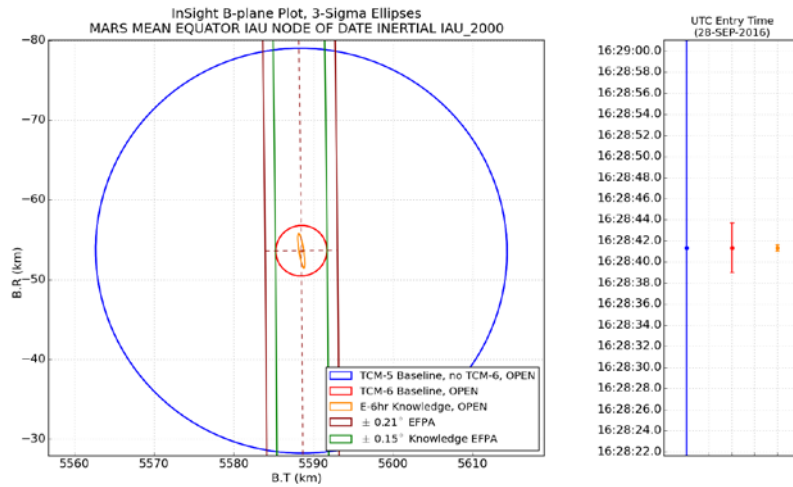


Figure 8. TCM-5 Delivery, TCM-6 Delivery/Knowledge B-plane Error Ellipse, and Entry Time Uncertainty (Baseline, Open)

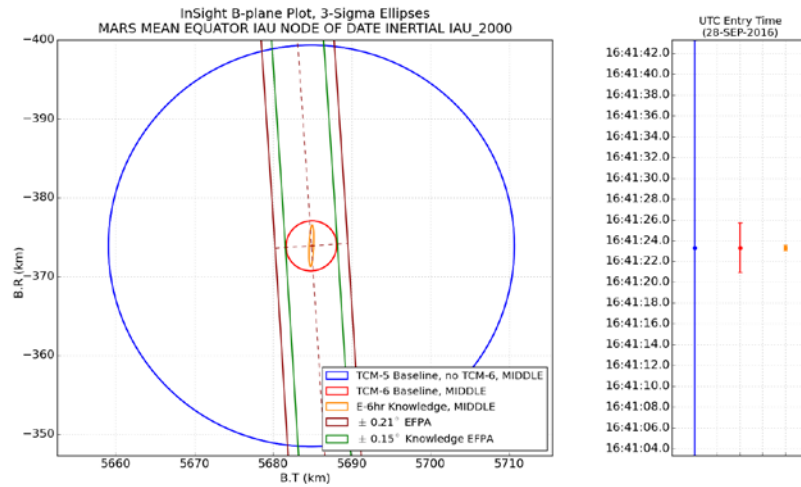


Figure 9. TCM-5 Delivery, TCM-6 Delivery/Knowledge B-plane Error Ellipse, and Entry Time Uncertainty (Baseline, Middle)

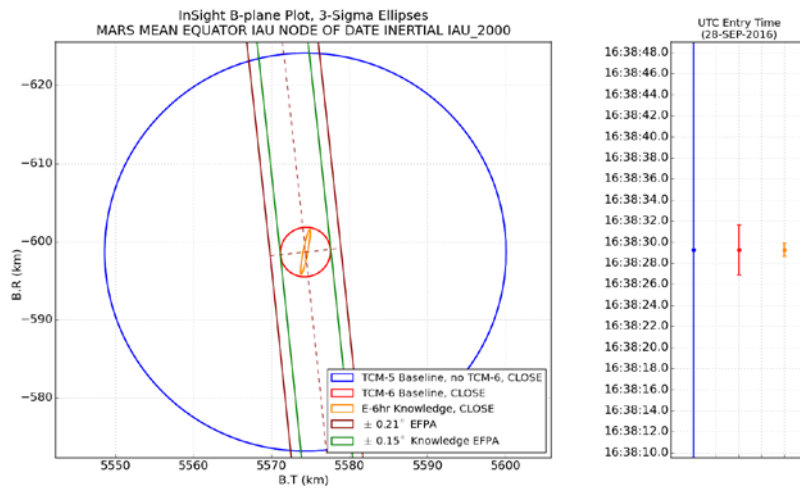


Figure 10. TCM-5 Delivery, TCM-6 Delivery/Knowledge B-plane Error Ellipse, and Entry Time Uncertainty (Baseline, Close)

Launch Date	Launch Window	EFPA 3- σ Uncertainty (deg)				
		All Cases include Doppler and Range Data				
		No Δ DOR	DSN Δ DOR	DSN+ESA Δ DOR	DSN+JAXA Δ DOR	DSN+ESA+JAXA Δ DOR
03/04/2016	Opt - 60m	0.3314	0.2584	0.1502	0.1633	0.1475
	Optimal	0.3315	0.2585	0.1502	0.1634	0.1475
	Opt + 60m	0.3316	0.2585	0.1501	0.1633	0.1474
03/17/2016	Opt - 60m	0.3568	0.2576	0.1488	0.1616	0.1458
	Optimal	0.3570	0.2577	0.1488	0.1616	0.1458
	Opt + 60m	0.3572	0.2578	0.1488	0.1616	0.1458
03/30/2016	Opt - 60m	0.4027	0.2648	0.1514	0.1639	0.1482
	Optimal	0.4027	0.2647	0.1512	0.1637	0.1479
	Opt + 60m	0.4030	0.2649	0.1514	0.1639	0.1482

Table 6. TCM-6 EFPA Delivery 3 σ Uncertainty

Sensitivity to Filter Assumptions

A series of parameterized sensitivity cases for the Approach phase were analyzed in order to determine the effects of changes to data assumptions and modeling uncertainties on the delivery accuracy for TCM-6 EFPA. The “No Margin” case represents an optimistic scenario with the following assumptions: (1) actual performance is on par with other mission experience rather than at the level of the requirements, (2) all requested Doppler and range tracking passes are successful, and (3) all requested Δ DOR measurements are successful and delivered within the expected timeframe. The difference in results between the “No Margin” and the baseline cases quantifies the amount of margin included in the navigation design. The table includes the nominal assumptions labeled as “Baseline”, a degraded uncertainty for each parameter studied labeled as “Degraded” and an improvement over the baseline for each parameter studied labeled as “No Margin”. Figure 11 illustrates the history mapping of these three filter scenarios.

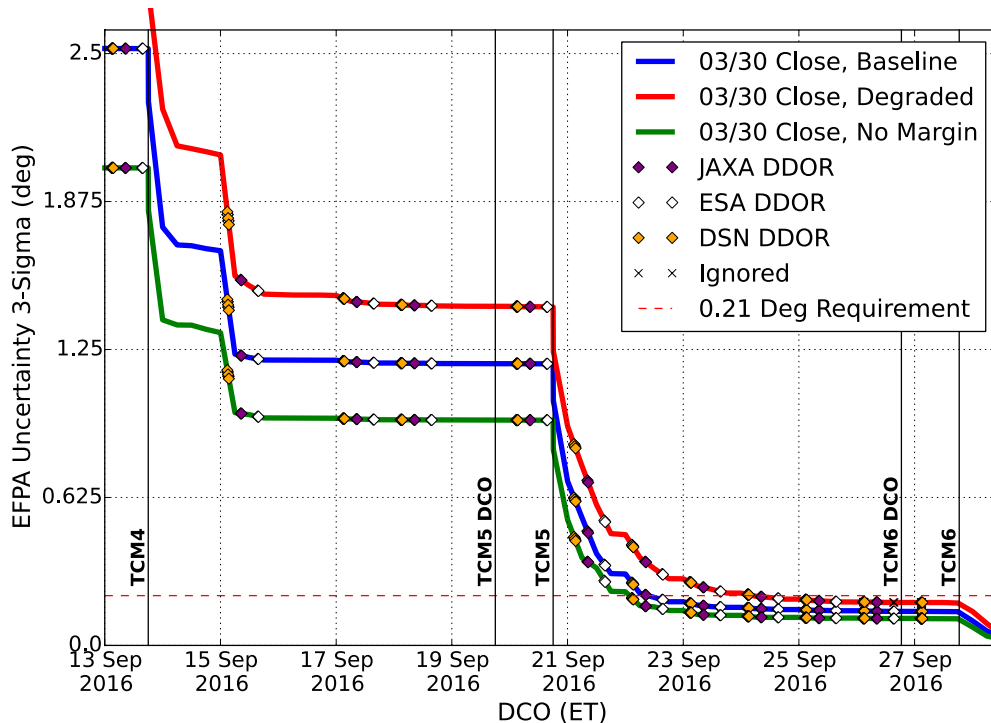


Figure 11. Baseline/No Margin/Degraded History Mapping

All three assumptions meet the EFPA requirement of 0.21 degrees (3- σ) with varying margin. Both “Baseline” and “No Margin” cases easily satisfy the EFPA requirement with 29% and 46% margin,

respectively. The “Degraded” case also meets the requirement about two days before TCM-6 with about 7% margin at the DCO.

Figures 12 and 13 show the EFPA history and associated B-plane error ellipses with respect to the Entry requirement. As illustrated in these figure, both JAXA and ESA Δ DORs improve the accuracy along the BdotR direction, which corresponds to the out-of-plane component. Note that for conservatism, the last available Malargüe Δ DOR before the TCM-6 data cutoff was ignored.

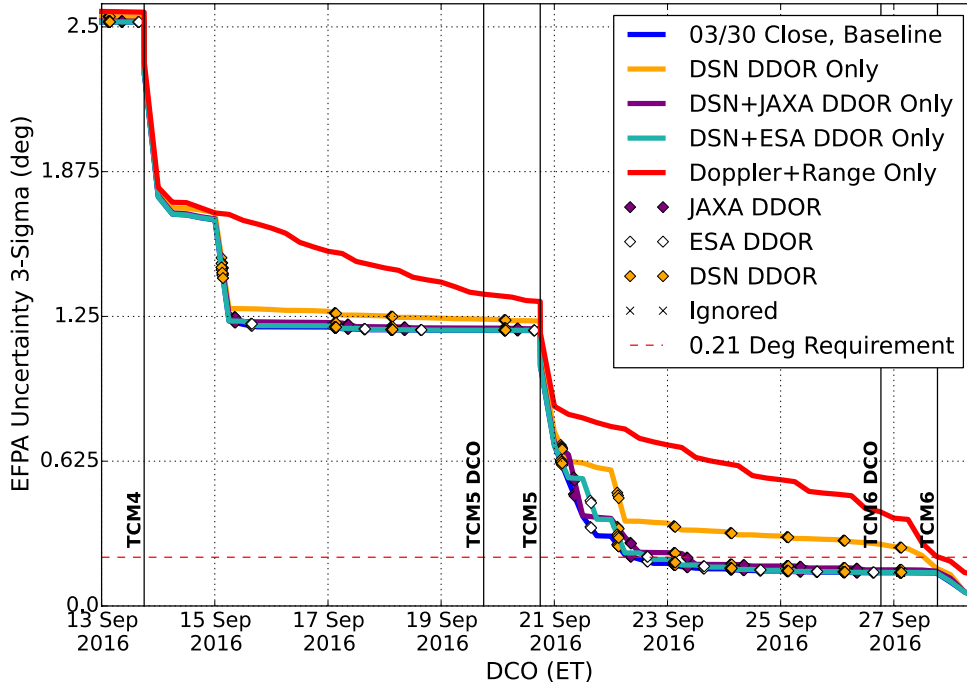


Figure 12. Δ DOR Sensitivity (EFPA)

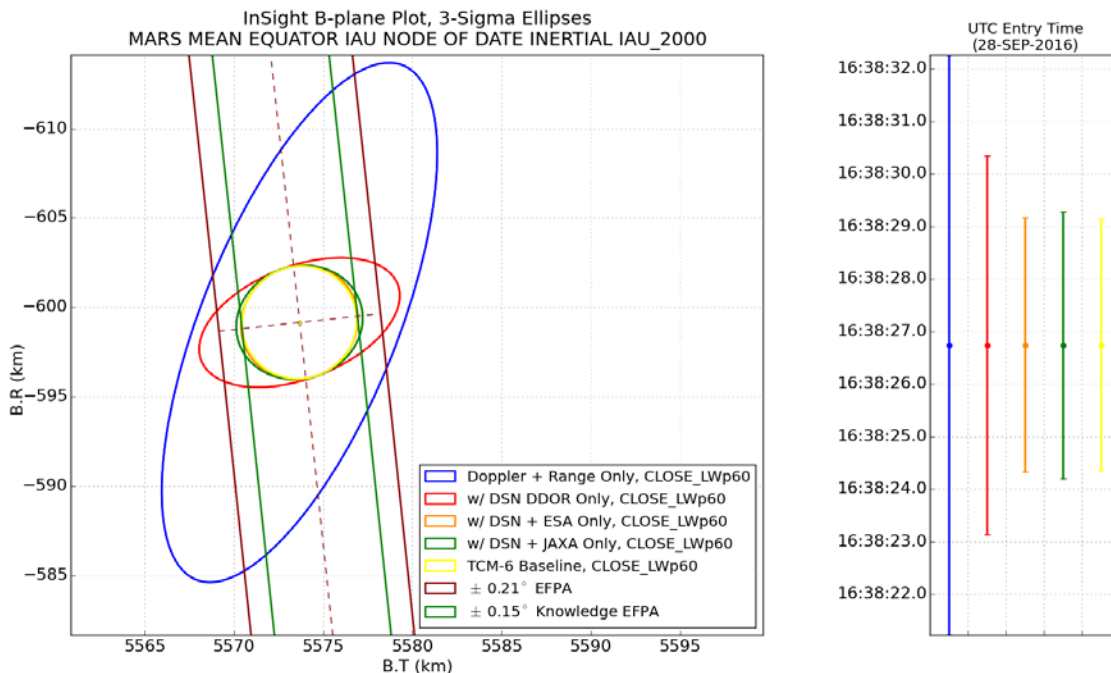


Figure 13. Δ DOR Sensitivity (B-Plane)

In conclusion, the delivery and OD accuracies are well behaved and sensitive to typical parameters such as dynamic uncertainties and data accuracy. The most significant sensitivities are caused by changes in TCM slew uncertainties and Δ DOR accuracy and latency. These results support the need for a robust understanding of the spacecraft GN&C uncertainties, a thruster calibration and a highly reliable Δ DOR system. By augmenting DSN Δ DORs with both ESA and JAXA Δ DORs, the navigation performance is robust to a loss of either one of the augmenting tracking networks.

Figure 14 shows the baseline delivery EFPA solution uncertainty for open, middle, and close of each launch opportunity; there is very little variation across both launch window and launch period. The launch opportunity at the close of the launch period, 03/30/16, corresponds to the largest EFPA uncertainty and is therefore presented as the stressing case.

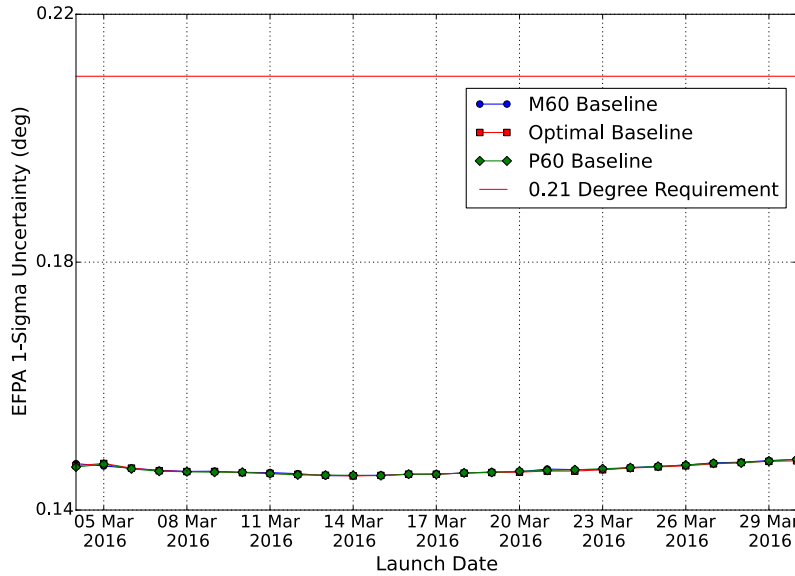


Figure 14. Baseline Delivery EFPA Uncertainty across the Launch Period

Trajectory Correction Maneuvers

InSight has scheduled six TCMs, while providing for back-up opportunities for TCMs 5 and 6. Mission Δ V requirements for these TCMs are estimated for each launch date by performing 5,000-sample Monte Carlo linear error analyses that model errors due to launch vehicle injection, orbit determination, and maneuver execution. The maneuver execution errors reflect the entire turn-burn-turn process as described in Table 7.

Δ V Magnitude	Fixed Magnitude Error	Proportional Magnitude Error	Fixed Pointing Error	Proportional Pointing Error
m/s	m/s	%	m/s per axis	rad per axis
0.04	0.00895	0.667	0.0135	0.00472
0.3	0.00895	0.667	0.0135	0.00472
1.5	0.00895	0.667	0.0135	0.02357
5	0.00895	0.667	0.0135	0.02357
≥ 20	0.00895	0.667	0.0135	0.00472

Table 7. Turn-Burn-Turn (1- σ) Maneuver Execution Errors

Table 8 summarizes the TCM Δ V performance for the open of the launch period. Launch vehicle targets are based on optimal performance for each launch day and are fixed during each daily launch window. This table shows the effects on Δ V estimates when launch occurs ± 60 min with respect to the optimal location for the open and close of the launch period. For each case the cost of TCM-1 is the dominant contributor, as it removes the launch vehicle target bias and injection errors. The data also show that TCM-2 is modestly affected by the time of launch within the daily window, while the remaining maneuvers (TCM-3

through TCM-6) are virtually unaffected. Figure 15 shows that the largest mission ΔV_{99} of 20.9 m/s occurs at the close of the daily window on 03/19/16. Each launch date meets the requirement that mission ΔV_{99} does not exceed 30 m/s.

TCM Schedule			TCM ΔV Statistics (m/s)						
TCM Relative Time	TCM Epoch (2016, UTC)	OD Data Cutoff	Launch Window	Determ ΔV	Mean ΔV	1σ ΔV	ΔV_{01}	ΔV_{99}	Cumulative ΔV_{99}
TCM-1 L + 10d	14 Mar 18:00 (Mon PDT)	TCM - 5d	Opt-60m	6.463	8.227	2.611	4.410	16.933	16.933
			Optimal	5.006	6.053	1.635	2.714	10.741	10.741
			Opt+60m	5.989	7.550	2.821	3.539	16.443	16.443
TCM-2 E - 156d	25 Apr 18:00 (Mon PDT)	TCM - 5d	Opt-60m	0	0.313	0.206	0.043	0.982	17.444
			Optimal	0	0.242	0.162	0.034	0.768	11.142
			Opt+60m	0	0.274	0.171	0.039	0.817	16.884
TCM-3 E - 45d	14 Aug 18:00 (Sun PDT)	TCM - 5d	Opt-60m	0	0.202	0.116	0.035	0.556	17.881
			Optimal	0	0.202	0.116	0.033	0.555	11.589
			Opt+60m	0	0.202	0.117	0.035	0.560	17.454
TCM-4 E - 15d	13 Sep 18:00 (Tue PDT)	TCM - 1d	Opt-60m	0	0.063	0.026	0.015	0.132	17.940
			Optimal	0	0.063	0.026	0.015	0.133	11.659
			Opt+60m	0	0.063	0.026	0.015	0.132	17.493
TCM-5 E - 8d	20 Sep 18:00 (Tue PDT)	TCM - 1d	Opt-60m	0	0.042	0.017	0.009	0.090	17.990
			Optimal	0	0.042	0.017	0.009	0.090	11.703
			Opt+60m	0	0.042	0.017	0.010	0.090	17.553
TCM-5X* E - 5d	23 Sep 18:00 (Fri PDT)	TCM - 1d	Any	0	No values calculated for TCM-5X				
TCM-6 E - 22h	27 Sep 18:38 (Tue PDT)	TCM - 24h	Opt-60m	0	0.170	0.075	0.036	0.378	18.192
			Optimal	0	0.170	0.075	0.036	0.380	11.904
			Opt+60m	0	0.170	0.075	0.036	0.379	17.710
TCM-6X* E - 8h	28 Sep 8:38 (Wed PDT)	TCM - 38h	Any	0	No values calculated for TCM-6X				
*contingency		TOTAL ΔV :	Opt-60m	6.463	9.301	2.685	5.322	18.192	-
			Optimal	5.006	7.056	1.700	3.553	11.904	-
			Opt+60m	5.989	8.586	2.886	4.427	17.710	-

Table 8. TCM DV Statistics for Launch Period Open (03/04/16)

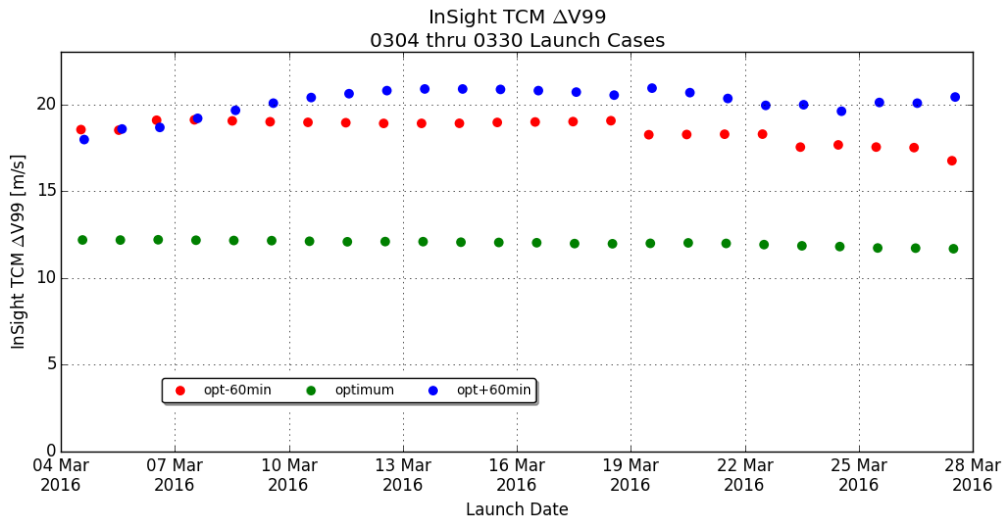


Figure 15. TCM DV99 Distribution across the Launch Period

50-Year Planetary Protection

The 99th percentile probability of impact for the open, middle, and close of the launch period are shown in Table 9. The worst-case probability of impact for the baseline mission (both MarCO spacecraft deploy) is 0.76×10^{-4} and occurs at the close of the launch window for a March 17th launch. The worst-case probability of impact for a one-MarCO deployment scenario is 0.71×10^{-4} . This occurs at the middle of the launch window for a March 19th launch. The worst-case probability of impact for a no-MarCO deployment scenario is 0.71×10^{-4} . This occurs at the open of the launch window for a March 20th launch. Since the maximum impact probability across the launch period for the different scenarios is 0.76×10^{-4} , the 50-year planetary protection requirement of 1.0×10^{-4} is satisfied.³

Launch Date	Launch Window	99 th Percentile Probability of Impact ($\times 10^{-4}$)		
		Both MarCO deploy	One MarCO deploys	No MarCO deployments
03/04/2016	Opt – 60m	0.69	0.68	0.69
	Optimal	0.69	0.69	0.69
	Opt + 60m	0.70	0.70	0.70
03/17/2016	Opt – 60m	0.69	0.69	0.69
	Optimal	0.69	0.69	0.69
	Opt + 60m	0.76	0.69	0.69
03/30/2016	Opt – 60m	0.69	0.69	0.69
	Optimal	0.69	0.69	0.69
	Opt + 60m	0.69	0.69	0.69

Table 9. Probability of Impact for Optimal Launch times

Non-Nominal Impact Probability

A non-nominal impact is defined as an impact that could result in the break-up of the spacecraft and re-release of terrestrial contaminants on Mars. Overall, non-nominal impact probability is the cumulative sum of the probability of non-nominal impact following each TCM. Table 10 shows the cumulative non-nominal impact probability for the open, middle, and close of the launch period. For each launch date, TCMs 1, 2, and 3 are the major contributors to non-nominal impact probability, driven by the larger $Q(i+1)$ values that reflect the longer times between TCMs early in the mission. The cumulative probability of non-nominal impact satisfies the requirement of 1×10^{-2} for each launch date.

Event	Location	03/04/16			03/17/16			03/30/16		
		P(i)	Q(i+1)	P(i)*Q(i+1)	P(i)	Q(i+1)	P(i)*Q(i+1)	P(i)	Q(i+1)	P(i)*Q(i+1)
Launch		0	7.36E-06	0	0	4.38E-06	0	0	4.38E-06	0
Injection		1.00E-04	7.11E-04	7.11E-08	1.00E-04	7.15E-04	7.15E-08	1.00E-04	7.17E-04	7.17E-08
TCM-1	L+10d	0.279	2.94E-03	8.19E-04	0.284	2.03E-03	5.76E-04	0.283	1.12E-03	3.16E-04
TCM-2	E-156d	0.000	2.03E-03	1.17E-12	0.000	2.03E-03	6.06E-12	0.000	2.03E-03	4.78E-12
TCAL	E-127d	0.581	5.72E-03	3.32E-03	0.588	5.72E-03	3.36E-03	0.587	5.72E-03	3.35E-03
TCM-3	E-45d	0.979	2.10E-03	2.05E-03	0.981	2.10E-03	2.06E-03	0.980	2.10E-03	2.06E-03
TCM-4	E-15d	1.000	4.90E-04	4.90E-04	1.000	4.90E-04	4.90E-04	1.000	4.90E-04	4.90E-04
TCM-5	E-8d	1.000	4.91E-04	4.91E-04	1.000	4.91E-04	4.91E-04	1.000	4.91E-04	4.91E-04
TCM-6	E-22h	1.94E-05	6.42E-05	1.25E-09	1.51E-05	6.42E-05	9.71E-10	2.16E-05	6.42E-05	1.38E-09
Cumulative Total:			7.18E-03		Total:	6.98E-03		Total:	6.71E-03	

P(i) : probability of impact after maneuver i

= total impact probability (100 km atmosphere) for all maneuvers except TCM-6

= probability of impact for non-nominal entry flight path angles for TCM-6

Q(i+1) : probability of not being able to execute maneuver i+1 given that maneuver i has occurred.

Table 10. Probability of Non-Nominal Impact for Optimal Launch times

LANDING ELLIPSE SIZE

Two methods were used to calculate the 99% ellipse size: (1) A Contour method that contains exactly 99% of the landing points, and (2) a Gaussian method which assumes that all landing points are Gaussian-distributed along each axis. The advantage of the Contour method is that requires no assumptions about the probability of the distribution of landing points; however, it is sensitive to the sample size (the ellipse size can vary significantly for a “small” number of landing points). The Gaussian method is typically well behaved; however, the 99% of the Gaussian ellipse may not contain 99% of the landing points. The landing footprint size for the open, middle, and close of the launch period is shown in Table 11.

Launch Date	Azimuth (deg)	Contour Method		Gaussian Method	
		99% Along-track* (km)	99% Cross-track** (km)	99% Along-track* (km)	99% Cross-track** (km)
03/04/16	79.8	121.7	26.4	130.3	28.3
03/17/16	89.0	115.3	25.5	124.2	27.6
03/30/16	95.5	117.9	26.1	124.8	27.7

*Along-track variability: 4.7 km 3s (Contour), 3.0 km 3s (Gaussian)

**Cross-track variability: 1.0 km 3s (Contour), 0.6 km 3s (Gaussian)

Table 11. Landing Footprint Size

CONCLUSIONS

This paper has summarized the launch/arrival strategies, the Navigation and Maneuver Design, and presented results to demonstrate that all InSight Mission Design and Navigation requirements are satisfied. This strategy consists of a 27-day launch period that provides EDL communications via UHF to MRO or Direct-To-Earth. Six trajectory correction maneuvers (TCMs) are planned in order to achieve the required entry delivery accuracies.

ACKNOWLEDGMENTS

The research described in this paper was carried out at the Jet Propulsion Laboratory, California Institute of Technology, under a contract with the National Aeronautics and Space Administration. The author would like to acknowledge the members of the InSight Team who contributed to the analyses that are reported on in this paper: Gene Bonfiglio, Min-Kun Chung, Matt Golombek, Tim McElrath, Max Schadeegg, and David Skulsky. The author also acknowledges the contributions of the GNC team at Lockheed Martin. Roby Wilson and Ralph Roncoli served as reviewers for this paper and provided useful comments. © 2016 California Institute of Technology. Government sponsorship acknowledged.

REFERENCES

- ¹ F. Abilleira, R. Frauenholz, K. Fujii, M. Wallace, T.H. You, “2016 InSight Mission Design and Navigation”, 24th AAS/AIAA Space Flight Mechanics Meeting, Santa Fe, New Mexico, Jan 26-30, 2014.
- ² M. Golombek, L. Redmond, H. Gengl, C. Schwartz, N. Warner, B. Banerdt, S. Smrekar, “Selection of the InSight Landing Site: Constraints, Plans, and Progress”, 44th Lunar and Planetary Science Conference (2013), The Woodlands, Texas, March 18-22, 2013.
- ³ M. Wallace, “Massively Parallel Bayesian Approach to Planetary Protection Trajectory Analysis and Design”, 2015 AAS/AIAA Astrodynamics Specialists Conference, Vail, Colorado, August 9-13, 2015.